FUSION PLASMAS

CONTROLLED FUSION

For half a century, scientists and engineers working in labs scattered around the globe have labored to turn the promise of controlled fusion energy into a practical reality (1–3). In fusion reactions, nuclei of light elements join to form heavier elements releasing enormous quantities of energy. Nuclear fusion powers the sun and other stars and is responsible for creating all the elements of the periodic table out of the "primordial soup" of protons and neutrons. The advantages of fusion energy seem clear enough: It offers the prospect of inexhaustible energy with few of the environmental drawbacks associated with fossil fuels or nuclear fission. The quest has been challenging: The problem of controlled fusion has turned out to be much more difficult than anyone had imagined. Progress has been steady, however, with recent experiments generating almost 20 MW of fusion power for extended periods (4,5), and workers in the field are confident that a fusion device can be built which could produce power at levels comparable to conventional power plants. The remaining questions concern the technological practicality and economic viability of current approaches. This is not to say that the problems that remain are "simply" a matter of engineering. Further progress will require the continued coevolution of experimental science, theory, and technology that has characterized the field since its inception.

The reactions of greatest interest for fusion energy involve deuterium (${}_1D^2$), a stable isotope of hydrogen whose nucleus contains one proton and one neutron:

$$ {}_1D^2 + {}_1D^2 \Rightarrow {}_2He^3 + {}_0n^1 + 3.2\ \text{MeV} \tag{1} $$

$$ {}_1D^2 + {}_1D^2 \Rightarrow {}_1T^3 + {}_1p^1 + 4.0\ \text{MeV} \tag{2} $$

$$ {}_1D^2 + {}_1T^3 \Rightarrow {}_2He^4 + {}_0n^1 + 17.6\ \text{MeV} \tag{3} $$

Deuterium occurs naturally, making up about 0.015% of all hydrogen. Separating the deuterium present in a glass of water and fusing it in a reactor would produce energy equivalent to 250 gallons of gasoline. Tritium, ${}_1T^3$, is an unstable isotope, with a half-life of 12.3 years, and would be bred from reactions between fusion neutrons and lithium, another abundant element. The net result would be to burn D and Li, producing He neutrons and energy. Despite complications raised by the necessity of breeding tritium, Eq. (3) has the largest reaction rate and thus is the most likely candidate for a fusion reactor.

The potential to use these fusion reactions to produce power was recognized almost as soon as they were discovered. Speculation began in 1944 among scientists developing the atomic bomb at Los Alamos (1). By 1951, these discussions spawned experiments in the United States and Great Britain. The work was initially classified, as all atomic research was in those times. In the same period, a parallel effort was taking place in the Soviet Union, also within the secret confines of the weapons program. It soon became clear to scientists working on the project that the problem would not be solved quickly and that no particular military importance would be attached to its solution. The issue of declassification was debated by national governments for several years, with a favorable decision made in 1957. Contacts among scientists working on the project from various nations increased and culminated in a dramatic joint conference held in Geneva in 1958. All the nations involved in fusion research came together to compare experience and exchange information. Fully operational versions of some fusion devices were put on display along with large-scale models of others. Despite the Cold War, which raged for another 30 years, controlled fusion research became a model for cooperation between otherwise hostile blocs.

Requirements for Fusion Energy

The basic requirements for a fusion reactor follow from the nuclear physics of the reactions. Figure 1 shows cross sections for the processes listed above versus the kinetic energy of an incident nucleus. The reaction rates peak at energies above 100 keV and are negligible below 5 keV. A comparison of cross sections with those for coulomb (elastic) scattering is also shown. Unlike the scattering rate, which diverges at low temperatures, the fusion rates peak at very high temperature and are always smaller by at least a factor of 10. This last fact means that even at the optimum temperature, around 30 keV for the deuterium–tritium reaction, nuclei must collide and scatter many times before they are likely to fuse. (In the plasma sciences, temperatures are usually measured in electronvolts; $kT = 1$ eV is equivalent to 11,600°C.) At these temperatures, matter is ionized into its ion and electron components, becoming a substance called plasma. In order not to lose the energy invested in bringing the nuclei to these high energies, it is necessary to confine the plasma for multiple scatterings during the time it takes for them to fuse.

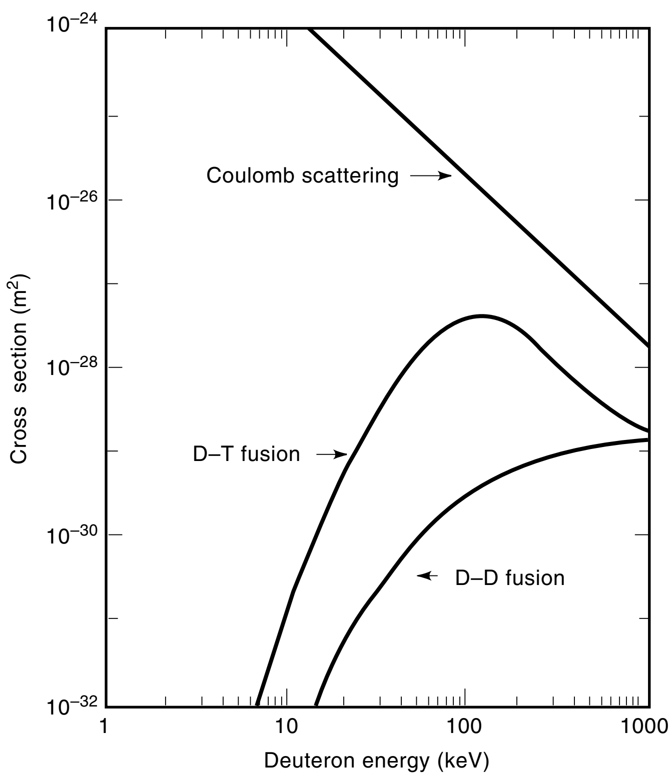

Figure 1. Cross sections for fusion reactions are shown and compared with the cross section for Coulomb scattering. The fusion curves peak at very high energies showing that high temperatures are required for fusion energy, At these temperatures, ordinary matter is ionized becoming a plasma. The cross section for elastic scattering is larger than that for fusion, even at the peak of the fusion curve. For a practical fusion energy device, the plasma must be confined for times long compared to the scattering time.

Plasmas are ubiquitous in nature, making up virtually all of the visible universe. Stars, the aurora, lightning, and neon lamps are all examples of plasmas, though they differ enormously in their temperature and density. Plasmas represent a fourth state of matter; if heat is added to a neutral gas, its temperature will rise until a point around 1 eV to 3 eV, where it begins ionizing. The phase transition is sharp; at only slightly higher temperatures the gas becomes a fully ionized plasma with new physical properties. Perhaps the most significant property that plasma has is that it is an excellent conductor of electricity. Strong currents can easily be induced to flow in plasmas, and they support a rich variety of electromagnetic and electrostatic waves.

In steady state, power input to the plasma must balance power outflow. The input power can be externally applied, as it is in present-day experiments, or can come from the fusion reaction itself. In most reactor schemes, charged fusion products (i.e., the alpha particle in DT fusion) would be contained and thermalized to heat the plasma, with the energetic neutrons used to drive a heat engine. Plasma losses can include thermal conduction and convection as well as various types of electromagnetic radiation. The most important radiation process is bremsstrahlung ("braking") radiation, which is generated whenever electrons accelerate as they do when they collide with other charged particles. Conductive and convective losses are analogous to heat transfer in ordinary materials, though details of the transport mechanism are quite different for plasmas. In fusion research, it is customary to define an energy confinement time:

$$\tau_E = W/P \tag{4}$$

where W is the total kinetic energy stored in the plasma, and P is the power flowing out via conduction and convection. Lawson (6) showed that elementary power balance led to two separable requirements for net gain from a fusion reactor; these were a minimum ion temperature of about 5 keV and a density confinement time product ($n\tau_E$) of approximately 10^{20} s/m^3. Together they define a boundary for "breakeven" shown in Fig. 2. The temperature requirement was first met in 1978 on the PLT tokamak (7) and the confinement figure exceeded in 1983 on Alcator C (8), while later experiments have approached the combined requirements (9–11). The Lawson criteria define the minimum performance for a fusion device to generate net thermal power. For a practical device, the power required to run the plant must be considered along with the inevitable losses that thermodynamics imposes whenever heat is converted to other forms of energy. It is also desirable if the energy to sustain the plasma comes entirely from charged fusion products. In this case, no external power source is re-

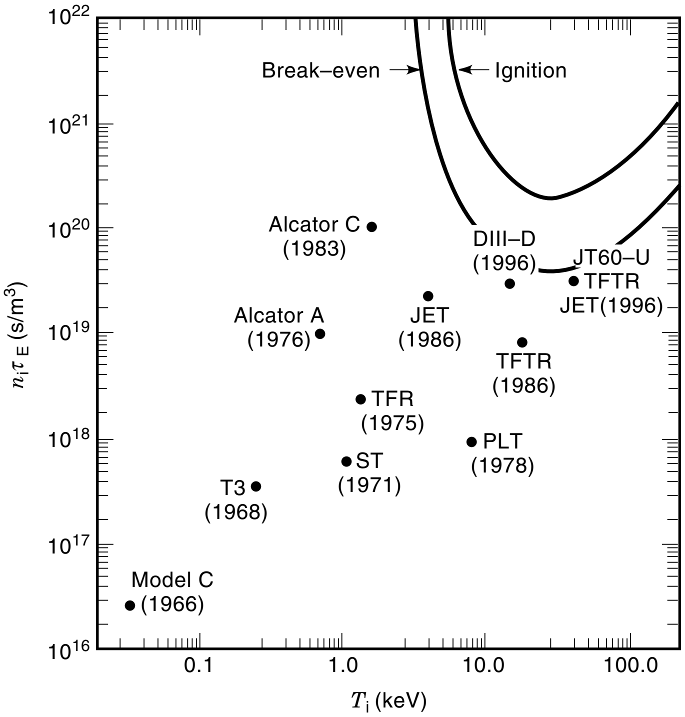

Figure 2. The requirements for net energy gain and for ignition are shown. Good confinement and high temperatures are both required. Results from various experiments are shown, along with the dates that the results were achieved. In current experiments, fusion power output has reached 20 MW, only slightly lower than the power input.

quired and the plasma "burns" as long as fuel is supplied. The requirements for this condition, called ignition, are more stringent than the breakeven requirements as can be seen in Fig. 2.

Plasma Confinement

The requirements for fusion described above are mathematically separable; however, in practice, both are linked to a single parameter, namely, confinement. Perfect confinement would be a state where heat and mass transfer were reduced to zero. To understand why confinement is so important, consider a simple analogy, namely, heating a house. The goal is to attain a given temperature inside, perhaps 20°C, while heat is lost to the colder outside world. The better the house is insulated—that is, the more efficiently the heat is confined within the house—the less fuel is consumed. The analogy is imperfect of course: An ordinary furnace will function even in a cold house, but the nuclear furnace only works when it is very hot. Of course, ordinary insulation is no help at all when trying to confine a plasma at temperatures approaching 100,000,000°C.

There are three ways to confine hot plasmas. The immense gravitational force of a star's mass can overcome the natural tendency of hot particles to fly apart. For such a huge object, the ratio of volume, in which energy is produced, to surface area, at which it is lost, is immense. Confinement in these systems is so good that the fusion reactions can proceed at very slow rates and still keep up with losses. Energy is produced by nuclear fusion in the core of the sun at a rate somewhat lower (per unit volume) than is produced by metabolism in the human body. Unfortunately, gravity is such a weak force that objects much smaller than the sun won't ignite. In a hydrogen bomb, a scheme called inertial confinement is employed. The fuel is heated and compressed by a fission explosion; the plasma is effectively confined by its own inertia and burns in less than a nanosecond. Of course, a hydrogen bomb is an example of uncontrolled fusion energy and is of no use for generating electricity. Researchers have instead attempted to use intense laser or ions beams to compress tiny pellets of fuel with the goal of producing fusion microexplosions. While most of this work has a military goal, that of exploring the physics of extremely high-density plasmas and validating computer codes which attempt to simulate nuclear weapons, it is possible that inertial confinement could be employed for energy production. The last approach for confining plasmas is by the use of strong magnetic fields; most of the research dedicated to fusion energy over the last 50 years has been in magnetic confinement.

Magnetic confinement relies on the fact that magnetic fields exert a force on ionized particles which is perpendicular to their direction of motion:

$$\boldsymbol{F} = m\frac{d\boldsymbol{v}}{dt} = Ze(\boldsymbol{E} + \boldsymbol{v} \times \boldsymbol{B}) \tag{5}$$

where v is the velocity of the particle in meters per second, m is its mass, the charge on an electron is $-e$, Z is the net ion charge in units of e, and B is the strength of the magnetic field in tesla. The solution to this equation, called cyclotron or gyro motion, has circular orbits in the plane perpendicular to B; the radius of the gyro orbit is given by the expression

$$\rho_c = \frac{mv_\perp}{ZeB} \tag{6}$$

The magnetic field has no effect on parallel particle motion so the full orbits are helical, with particles spiraling around magnetic field lines, and are effectively confined by them to within one gyro radius (Fig. 3).

To confine high-temperature plasmas, whose particles have thermal velocities in the range of 10^6 m/s or charged fusion products that have velocities 10 times higher, in devices with finite size, strong magnetic fields are required. Experimental devices employ fields in the range of 1 T to 10 T;

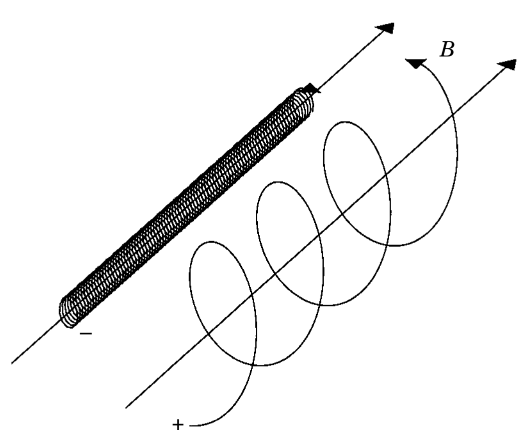

Figure 3. Cyclotron or gyro motion for ions and electrons in a straight uniform field. The particles are confined in the plane perpendicular to the field but are unconfined parallel to it.

for comparison, the earth's magnetic field is on the order of 5×10^{-5} T. A deuterium plasma ion at 10 keV in a field of 5 T has a gyro radius ~3 mm.

In a configuration like that shown in the figure, particles would be well-confined in the directions perpendicular to the magnetic field, only crossing field lines as the result of collisions. Unfortunately, this configuration, which could be produced by a simple solenoidal coil, provides no confinement at all in the direction parallel to the magnetic field and hot plasma particles would stream freely out the ends. A variety of ideas for eliminating the end losses have been tried, but without much success. A more promising approach is to get rid of the end losses by getting rid of the ends, bending the field lines into closed circles (Fig. 4).

The resulting geometry is a torus, a donut shape, which is defined when a circle or other two-dimensional shape is rotated about an axis lying in the same plane. This is, in essence, the approach used in most magnetic confinement experiments; however, the resulting physics is anything but simple. While particles are well-confined on straight magnetic field lines, they quickly drift off when the lines are curved. This particle drift can be canceled by introducing a "rotational transform"—that is, by twisting the magnetic field lines as they circle around the central axis. A few definitions are useful at this point. The long way around the donut is called the toroidal direction, and the short way around is referred to as the poloidal direction. A quantity, q, is defined which is equal to the number times a field line circles in the toroidal direction for each time it circles in the poloidal direction. The magnetic field that we have been discussing so far is purely in the toroidal direction. The rotational transform is produced by a magnetic field in the poloidal direction. The two fields, when combined, form helices that wrap around the torus; the particles unrestrained motion parallel to the field is also helical. Since the particle drifts are vertical (with the torus oriented as in Fig. 4), they alternately drift toward the minor axis of the torus and away from it as they circle, cancelling the drifts on average. The poloidal fields that create the rotational transform can be generated by external magnets or from currents flowing toroidally in the plasma itself. A nearly infinite variety of toroidal devices are possible from these basic components. Some have been successful and are the subject of continuing research, while others have been abandoned as false starts. Later sections will describe some of the more promising schemes.

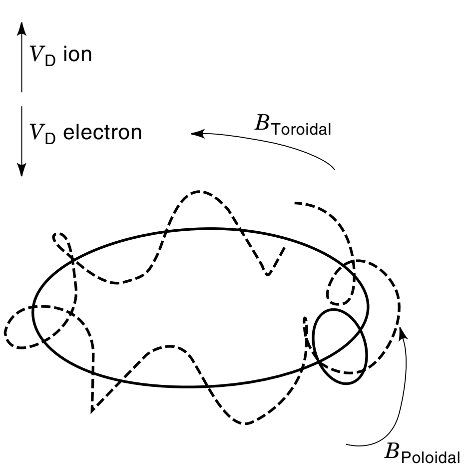

Figure 4. End losses can be eliminated by curving the simple solenoid shown in Fig. 3 into a torus. A second component of the field is required to cancel the vertical drifts that particles experience in this geometry.

Confinement of individual particles is a necessary but not sufficient condition for magnetic confinement. Plasmas can be thought of as electrically conducting fluids, capable of carrying current and exhibiting collective behavior, like waves. At sufficient pressure, and at the densities and temperatures necessary for fusion, plasmas exert considerable pressure; these collective effects can generate magnetic fields that compete in strength with those confining them. Unless great care is taken to create a stable configuration, the plasma can, in effect, push aside the bars of its magnetic cage and escape. A later section on magnetohydrodynamics (MHD), will elaborate on this topic.

Confinement Experiments

In such a small space, it would be impossible to do justice to the myriad of approaches to magnetic confinement that have been taken over the years. This section will review a handful of the more prominent schemes. The reader is referred to the bibliography for more detail.

Stellarators. One of the earliest magnetic confinement schemes was the stellarator, invented by Lyman Spitzer in 1951 at Princeton University and named after the stars that it was designed to emulate. The earliest versions created the necessary rotational transform by literally twisting the torus into a figure-eight configuration. A plasma was formed in this oddly shaped vacuum vessel that was surrounded by solenoidal electromagnets. This approach was soon discontinued in favor of machines with toroidal plasmas and a magnetic transform generated by helical windings. Experiments continued at Princeton and at other labs throughout the 1950s and 1960s, but met with only modest success. Electron temperatures achieved never exceeded 50 eV and confinement times were no more than a few milliseconds (12). During this period, the science of plasma physics was developing quickly, however, the intrinsic three-dimensional geometry of the stellarator made accurate calculations of its properties impossible at the time. The lack of good confinement in stellarators was attributed to plasma instabilities, and the approach was all but abandoned as promising results from the Russian-invented tokamak were disseminated. Groups at Kyoto University and the Max Planck Institute in Germany continued work on stellarators on a smaller scale, while theory and computers advanced to the point where they could tackle three-dimensional problems. Scientists recognized that great care needed to be taken in the design and construction of stellarator coils. The poor results of earlier machines were attributed to field errors coming from imperfect coils. By the 1980s, stellarators were producing plasmas with temperatures near 2 keV and with confinement times up to 30 ms, only slightly worse than tokamaks of similar size (13,14). Since stellarators have a natural ability to operate in steady state (tokamaks, the most developed confinement device, tend to work in pulsed mode), these results generated great interest and prompted the construction of more ambitious experiments. Currently two very large stellarators are under construction.

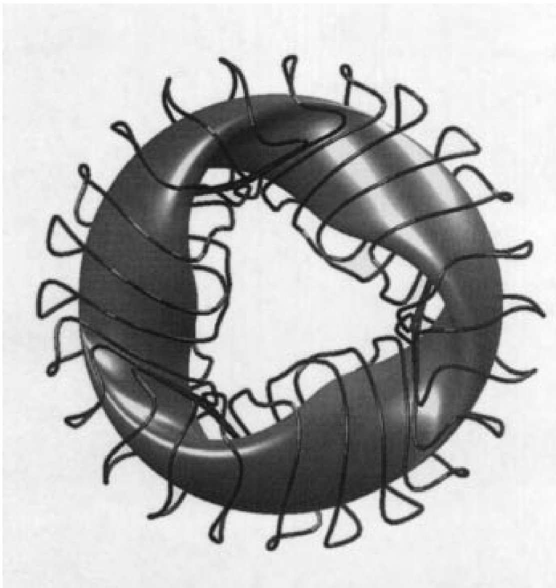

Figure 5. A computer model of an advanced stellarator designed at the Oak Ridge National Laboratory. The large shaded torus represents the plasma surface which is surrounded, in turn, by the 24 magnet coils which are used to create it. The coil shapes allow them to carry both toroidal and poloidal currents. This so-called modular design allows design of a stellarator which would be easier to construct and assemble.

In Japan, the large helical device (LHD) will begin operation late in 1998; and in Germany, Wendelstein 7-X is scheduled to begin experiments about 4 years later. Both machines have major diameters over 10 m, more than twice the size of existing facilities, and are designed to test the scaling of stellarator physics to reactor like conditions. Figure 5 is a computer model of an advanced stellarator, showing the complex coil shapes required for these devices.

Tokamaks. Parallel to stellarator development was the exploration of the tokamak in the Soviet Union. The acronym tokamak stands for *toroidalnaya kamera magitnaya katushka* or toroidal chamber and magnetic coil, a device invented by Igor Tamm and Andrei Sakharov (perhaps best known for winning the Nobel Peace Prize for his work on human rights). The early Russian work may have been inspired, in part, by information gathered from the British nuclear laboratory at Harwell. Scientists at Harwell had been working with a class of devices called "pinches," named after the pinching force that a current carrying plasma exerts on itself. Regardless of its origin, the tokamak was a marked improvement over the existing pinches. In addition to the pinching fields, provided by toroidal plasmas currents, the tokamak added a very strong toroidal field to stabilize the plasma. Soon results from tokamak experiments far exceeded those from any other fusion experiment. Plasmas with electron temperatures near 1 keV, ion temperatures of 300 eV and densities over 5×10^{19} were reported from the T3 tokamak at the Kurchatov Institute in Moscow (15). Energy confinement times were up to 10 times better than the best stellarator results. Scientists outside the Soviet Union were at first skeptical of the claims; the plasma diagnostics available at the time were rudimentary and the results seemed too good to be true. A second dramatic moment in the development of fusion energy came in 1969 when a team of British scientists traveled to the Kurchatov and used a newly developed laser scattering diagnostic to verify the Russian claims (16). The impact of this measurement rolled over the international fusion community like a thunderclap. Almost overnight, plans for new tokamaks were laid at all the major labs.

The early tokamaks were relatively simple devices. A toroidal vacuum vessel was surrounded by a solenoid to produce the strong toroidal magnetic field. Threaded through the hole in the torus was an iron core, which, when powered by external windings, became the primary for an enormous step-down transformer. When current in the external windings was changed, a toroidal electric field was produced that was parallel to the magnetic field. A small amount of hydrogen that had been introduced into the vacuum chamber was quickly ionized as electrons were accelerated by the electric field. Soon a substantial current was flowing in the plasma, generating the poloidal field that provided the rotational transform. The plasma current also provided a source of heat as electrons, accelerated in the electric field, collided with the relatively stationary ions. Like the heating of a filament in an electric lightbulb, this process converts electrical energy to heat. These devices easily produced plasma temperatures in the range 100 eV to 1000 eV with confinement times of several milliseconds. Later, tokamaks replaced the iron core with an air core transformer, added additional forms of heating, and increased the size of the machine dramatically. The main coils of today's large tokamaks stand 4 m high and have vacuum vessels large enough for a man to walk around in. These machines produce temperatures up to 40 keV and confinement times on the order of 1 s. The JT-60 tokamak in Japan has produced plasmas that are at the point of scientific breakeven (9), though they are run only in hydrogen and deuterium and do not produce substantial fusion power. The TFTR tokamak (Tokamak Fusion Test Reactor) in the United States and JET (Joint European Torus) in England produce similar plasmas and have been run with deuterium–tritium fuel. These devices produced 10 MW and 20 MW of fusion power, respectively (5,11). Researchers have learned how to optimize confinement in tokamaks, at least transiently, almost entirely eliminating the microinstabilities that normally drive transport in plasmas (17–20). Figure 6 shows the DIII-D tokamak in its test cell at General Atomics in San Diego.

Other Toroidal Confinement Schemes. The reversed field pinch (RFP) first developed at Harwell, England in the late 1950s (21), is an axisymmetric device similar in many ways to the tokamak. It evolved out of work on toroidal versions of the stabilized Z pinch (see below). Like the tokamak, a poloidal field is produced by toroidal current flowing in the plasma and a toroidal field produced by external coils. However, in the case of the RFP, the two are of roughly equal strength and, most significantly, the toroidal field is reversed near the plasma edge, producing a "minimum energy" equilibrium that is particularly stable to certain MHD modes. In principle, the RFP can confine plasmas with a higher ratio of plasma pressure to magnetic pressure than stellarators or tokamaks. The field reversal can be obtained spontaneously or by programming the external currents, using the low resistivity of the plasma to freeze-in the field. The field reversal is sustained

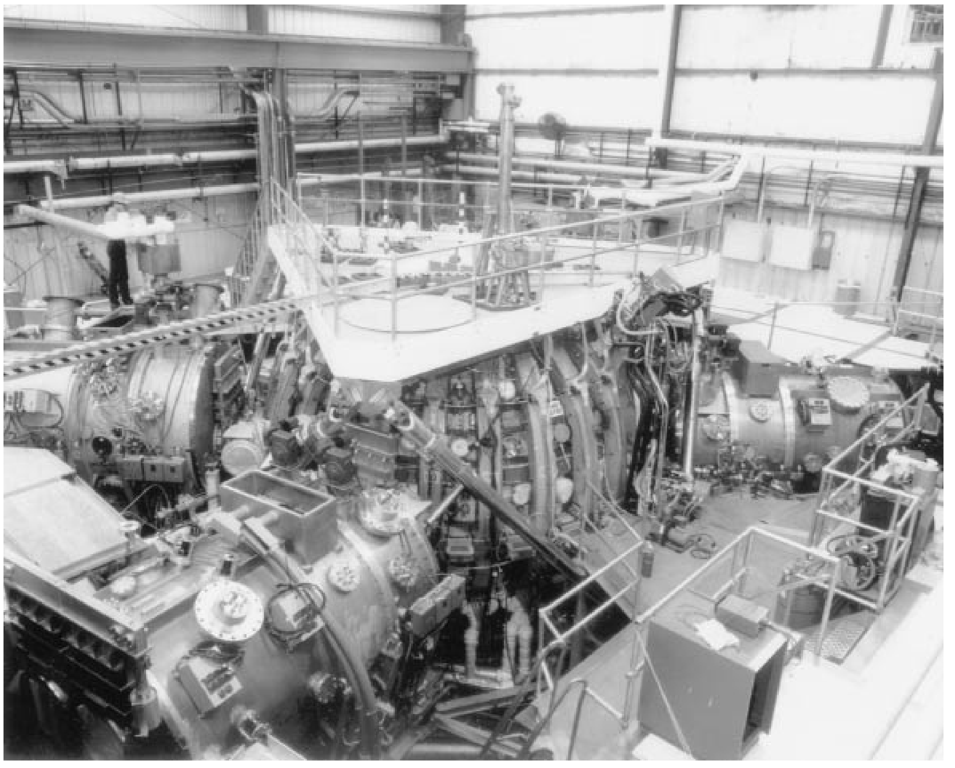

Figure 6. The DIII-D tokamak was built by General Atomics in San Diego. The tokamak, which is in the center of the photograph, is surrounded by neutral beam heating sources (the three large cylindrical chambers) and various diagnostic equipment. The most notable feature of the tokamak is its large toroidal magnetic field coils. The scale can be estimated from the technician standing in the upper left of the photo.

against resistive relaxation by a magnetic dynamo, where motion of the conductive plasma is converted to magnetic field energy, a process similar to the one that produces the earth's field. Research on RFPs is continuing, with emphasis on transport and magnetic turbulence (22).

Another family of confinement devices is the compact torus. Devices of this type attempt to create a configuration in a minimum energy state with respect to gross MHD stability. The torus-shaped plasmas do not encircle any coils (as they do in the tokamak, stellarator, or RFP), a significant engineering advantage for a reactor where stresses and heat loads on the inner cylinder of conventional toroidal devices can limit machine performance. Like the RFP, these devices should be capable of confining high pressure plasmas. Two variants exist: the spheromak, which has both toroidal and poloidal fields in a force free configuration (the plasma current is everywhere parallel to the magnetic field), and the FRC or field reversed configuration, which has only poloidal fields. Both have been produced only in short pulsed experiments that have concentrated on creation and verification of the basic equilibrium (23).

Linear Systems. While it was clear that end losses would make simple linear devices unsuitable for reactors, many early experiments were carried in this geometry to test the basic principles of magnetic confinement. Two basic types of schemes were tested: the theta pinch and the *Z* pinch. Cylindrical in shape and named after the direction of the induced current in the standard coordinate system, these devices were operated in short pulses; end losses rapidly drained particles and energy from the plasmas that were created. Work on *Z* pinches actually predated controlled fusion research (24). At Los Alamos in 1951 and somewhat later at the Lawrence Berkeley Lab in California, researchers used capacitor banks and low induction coils to compress plasmas to very high densities. In machines built after 1956, a small axial field was introduced that had the effect of somewhat reducing instabilities, but also lowered the density of the plasma produced. This so-called "stabilized *Z* pinch" was the ancestor of the tokamak and the RFP. The theta pinch was also studied extensively at Los Alamos, starting in 1958. The experiments had a low-inductance single turn coil in the theta direction, allowing current in the machine to be pulsed at very high rates. The resulting plasma was heated and compressed by a shock wave that propagated inward toward the machine axis and allowed production of very high densities ($\sim 10^{22}/m^3$) and ion temperatures ($\sim$1 keV) (25). Because of their low mass, electrons did not pick up much energy from the shock and remained much colder. Attempts to produce a toroidal version of the theta pinch could never overcome MHD instabilities, and the approach was eventually abandoned.

At the Lawrence Livermore Lab, researchers began working on an idea that they hoped would allow them to plug the end losses in linear machines (1). This idea was the magnetic mirror, in which plasma particles are reflected by converging magnetic fields produced by high-field coils added to each end of a simple solenoid. The mirror works by exploiting the principle of adiabatic invariance; which will be described in a later section. It is the same phenomenon that causes charged particles from the solar wind to be trapped in the earth's dipole field: the radiation or Van Allen Belts (26). The simple mirror was shown to be unstable by Ioffe et al. (27), who suggested an improvement, the minimum *B* mirror, an idea that was incorporated into all later experiments. Plasmas in a minimum *B* mirror were confined by coils shaped like the seam of a baseball and spread out in two large fans. Because mirror plasmas were confined by external fields only, they held out the prospect for steady-state operation. Their open fieldline geometry was seen as a virtue; it was proposed that energy from charged fusion products, many of which would be lost out the open lines, could be converted directly to electricity, bypassing the inherently inefficient thermal cycle upon which all conventional power generation is based. A magnetic mirror only traps particles whose motions are mainly perpendicular to the magnetic axis. Those with mostly parallel energy are rapidly lost. To maintain this highly non-Maxwellian velocity distribution, a mirror machine would have to run in a regime where collisions were rare. In the end, microinstabilities doomed this approach and despite a host of inventions to improve the concept, the mirror never succeeded in achieving good confinement for thermal plasmas (28).

Plasma Wall Interactions

Eventually, all the energy and power that is put into the plasma and all the energy from charged fusion products must come out onto an ordinary material surface. It is a measure of progress that these fluxes are now a major concern for fusion experiments. Hot plasmas were once thought of as fragile things, extinguished by even the lightest touch of material objects. Now, with plasma energies over 10 MJ, it is the material objects that are at risk. Plasma facing components must be carefully designed to avoid melting and vaporization. It is also necessary to prevent impurities from entering the plasma. Impurities, particularly low-Z ions like carbon or oxygen, can dilute hydrogenic fuel and reduce fusion rates. High-Z ions, from the vacuum vessel structure, are not fully ionized even at high temperatures and can radiate copiously and may be a significant energy loss channel. To minimize impurity generation in modern experiments, all components that come into contact with the plasma are usually made of refractory materials like graphite, molybdenum, or tungsten. Heat loads are not the only process which can generate impurities. Energetic ions can remove atoms from a surface directly, by a process called sputtering, even if the average heat load is too low to vaporize material in bulk.

Serious attention must be paid to the design of the structures that form the plasma boundary and that will take the largest heat and particle loads. There are two approaches to this problem: limiters and divertors (29). A limiter is simply a solid object put into direct contact with the plasma edge. Hot plasma on magnetic field lines that intersect the limiter quickly gives up its heat via parallel transport along the relatively short connection length. The limiter sets a boundary condition for the plasma with near zero temperature and density (at least compared to the core plasma). To provide sufficient “wetted” surface to absorb the heat loads, limiters must be made conformal to the plasma surface; even small mismatches can lead to localized heating and melting. In a divertor, by contrast, the magnetic field lines at the edge of the plasma are diverted into a separate chamber, where all plasma wall interactions can be isolated. There are a number of advantages to this approach. First, because the divertor plates are located away from main plasma, it is easier to keep any particles and impurities that are generated away from the plasma core. Second, the connection length along open field lines can be made quite long. This allows for a larger temperature gradient between the divertor and main plasma, reducing the effects of energetic ions at the contact point and easing the boundary condition imposed on the main plasma. Temperatures near the divertor walls can be a fraction of an electronvolt, while upstream temperatures, adjacent to the plasma, can be near 100 eV (30). Finally, neutral gas in the divertor chamber can be highly compressed, allowing impurities and helium ash from the fusion process to be efficiently pumped.

PLASMAS: BASIC PROCESSES

Although the underlying processes that determine plasma behavior are from well-understood branches of physics, classical electrodynamics, and classical mechanics, the behavior itself can be extremely complex. The motions (usually referred to as orbits) of individual particles are fundamentally important, however, plasmas are collections of enormous numbers of particles. A typical plasma fusion experiment may have over 10^{21} ions and electrons rendering a simple mechanical approach impossible. This is not only because of the large numbers of particles involved; even the dynamics of systems as simple as three mutually interacting charges cannot be solved exactly. Ensembles of plasma particles evolve chaotically; systems with almost identical initial conditions diverge exponentially over time. At best, only the evolution of macroscopic properties can be calculated. Because plasmas are typically dynamic and far from equilibrium, this approach requires the machinery of nonequilibrium statistical mechanics. Unfortunately, even with a statistical approach, most real-world plasma problems are intractable and require further approximations before they can be solved. Researchers develop the theory of plasmas by working out the simplest cases first, then gradually reducing the number and scope of the approximations as more realistic problems are tackled.

Quasi-Neutrality

An essential property of plasmas is quasi-neutrality, which means that the negative and positive electrical charges that make up a plasma are approximately balanced everywhere. Significant charge separation can occur only over a small scale, called the Debye length, defined by the balance between electrical and thermal forces:

$$\lambda_D \equiv \left(\frac{T_e}{n_e e^2}\right)^{1/2} \tag{7}$$

where n_e is the electron density in m^{-3}, T_e is the electron temperature in electronvolts, and e is the electron charge. The plasmas we deal with in controlled fusion are hot enough to achieve significant ionization and dense enough for λ_D to be much smaller than the plasma size. Electron thermal motions enforce quasi-neutrality on time scales longer than $\tau = \lambda_D/v_e$; thus ordinary electromagnetic waves cannot propagate in a plasma unless their frequency is higher than $1/\tau = v_e/\lambda_D \equiv \omega_{pe}$, the electron plasma frequency. (The reflection of radio waves off the ionosphere is a manifestation of this property of plasmas.)

Particle Orbits

Despite the intractability of a purely mechanical approach to plasma physics, it is still important to study the motion of individual particles in a plasma. First, the collective properties of plasmas are made of these motions, and they contribute strongly to its behavior. Second, fusion plasmas contain high-energy ions, including charged fusion products which interact only weakly with the background plasma and which can be well understood by studying their orbits. Particle orbits are determined by elementary mechanics and the interactions of charged particles with electric and magnetic fields shown in Eq. 5. As discussed above, the solution, for the case of a uniform B field with $E = 0$, is free and constant motion parallel to B and circular motion in the directions perpendicular to B. The circular motion is characterized by a frequency ω_c and a radius ρ_c given by

$$\omega_c = \frac{ZeB}{mc} \tag{8}$$

$$\rho_c = \frac{v_\perp}{\omega_c} = \frac{mv_\perp}{ZeB} \tag{9}$$

where $v_\perp$ is the component of the particle velocity perpendicular to the magnetic field and $v_\parallel$ is the parallel component. For a typical fusion plasma deuterium ion with a temperature of 10 keV in a field of 5 T, the cyclotron frequency, $\omega_{ci} = 2.4 \times 10^8$ and $\rho_{ci} = 2.9$ mm. For electrons at the same energy, the lower mass results in $\omega_{ce} = 8.8 \times 10^{11}$ and $\rho_{ce} = 0.047$ mm. In this case, both types of charged particles are confined onto the magnetic field lines to within a gyro radius. For nonuniform magnetic fields, electrons and ions drift off the field lines in opposite directions. The drift velocities, which are proportional to the particles' thermal velocity, are given by

$$v_d = \pm\frac{v_\perp \rho}{2}\frac{(\boldsymbol{B} \times \nabla \boldsymbol{B})}{B^2} \tag{10}$$

Note that for a simple toroidal solenoid we have $|B| \propto 1/R$ and $\nabla B \propto 1/R^2$, so $\boldsymbol{B} \times \nabla\boldsymbol{B}/B^2$ is just $1/R$. A drift of similar magnitude occurs when the magnetic field lines are curved. Because electron and ions drift in opposite directions, the motion can give rise to electric fields perpendicular to the magnetic field. These exist because the magnetic field inhibits the motion of electrons that would normally cancel the electric field. Electric fields can also cause electrons and ions to drift off of magnetic field lines, this time in the same direction and independently of their thermal velocity. This drift velocity is given by:

$$v_E = \frac{\boldsymbol{E} \times \boldsymbol{B}}{B^2} \tag{11}$$

Note that the particles continue to execute gyro orbits as they drift. Since the gyro motion is fast compared to drift motions and the gyro radius is small compared to other scale lengths, the gyro orbits are often averaged over for all subsequent analysis. Also of importance are so-called adiabatic invariants. These are quantities that are approximately conserved by particle orbits; the first and most important of these is $\mu \equiv mv_\perp^2/2B$. Charged particles can be reflected by converging magnetic field lines since μ conservation implies that perpendicular energy must increase as the field magnitude grows. To conserve energy, the additional perpendicular energy must come at the expense of parallel motion which is reduced to zero at a sufficiently high magnetic field. This is the principle behind the magnetic mirror discussed earlier.

Collisional Phenomena

As ions in a plasma approach each other, they are mutually repelled by the electrostatic force generated by the electric field that surrounds all charged particles. The interaction deflects the particles, scattering them elastically—that is, without any net change in the combined kinetic energy for the pair. The scattering angle is larger if the particles pass close to each other, or if the particles are moving slowly, which allows a longer period of interaction and for a larger relative effect of that interaction. The cross section for 90° scattering was first calculated by Rutherford in 1911:

$$\sigma_{90} = \frac{\pi e^4}{(4\pi\epsilon_0)^2 m^2 v^4} \tag{12}$$

The attractive force between unlike charges has a similar effect, with the scattering dynamics of electrons and ions differing only due to their different masses and velocities. Unlike collisions between neutral atoms, which are due to the very short-range forces induced by mutual polarization, the scattering of charged particles is inherently long-range. This means that multiple small-angle interactions have an accumulated effect that are more important than the relatively rare large-angle collisions. It was shown by Spitzer that in a plasma the scattering cross section is larger than σ_{90} by the factor $\log \Lambda$, the Coulomb logarithm, where $\Lambda \equiv \lambda_D \times mv^2/e^2 \propto \sqrt{(n/T^3)}$. λ_D appears in this expression because Debye shielding cancels the electrostatic field over larger distances. The scattering cross section for plasma particles is then of the order $\sigma \sim \sigma_{90} \log \Lambda$, with $\log \Lambda$ on the order of 15 for fusion plasmas.

With a collision cross section σ, a particle with velocity v will undergo collisions at a rate $\nu \equiv n\sigma v \propto n/(m^{1/2}T^{3/2})$, where n is the density of the background plasma. At equivalent energies, the faster moving electrons will collide more often by a factor $\sqrt{m_i/m_e}$. Collisions impede the ability of plasmas to carry current as the momentum of the charge carrying electrons is lost to the ions. Spitzer resistivity, appropriate for unmagnetized plasmas or for currents flowing parallel to the magnetic field, is given by Eq. (13). For a typical fusion plasma, at temperatures of 20 keV, the resistivity is about $100 \times$ lower than for copper:

$$\eta = 0.51\frac{m_e^{1/2}e^2 \log \Lambda}{3\epsilon_0^2(2\pi T_e)^{3/2}} \approx \frac{7.8 \times 10^{-4}}{T_e^{3/2}}\ \Omega \cdot \text{m} \tag{13}$$

A magnetic field alters the effects of collisions on a plasma. Since electrons and ions in a uniform magnetic field are tied to the field lines, a collision will move the particles at most by one gyro radius. A diffusion coefficient can be defined by

$$D = \frac{(\text{stepwise})^2}{\tau_{\text{collision}}} = \rho_c^2 v \approx \frac{nm^{1/2}}{B^2 T^{1/2}} \tag{14}$$

We note that in this simplified geometry, diffusion is inhibited by the magnetic field by a factor that is roughly the ratio of collision mean free path to the gyro radius squared. A magnetized plasma can be defined as one where this ratio is large. Diffusion is also reduced as plasmas grow hotter—a favorable result since the goal is to confine very hot plasmas. It is also worth remarking that in a magnetized plasma, ions, because of their larger gyro orbits, tend to diffuse faster than electrons, while in an unmagnetized plasma the opposite is true. Typically, electron dynamics will dominate transport parallel to the field, and ions will dominate in the perpendicular direction. Collisions between like particles, electrons and electrons or ions and ions, will not lead to particle diffusion since the net momentum is unchanged and the particles merely exchange positions. This is the same reason that electrical conductivity is governed by electron–ion collisions. Since the magnetic field does not affect parallel motions, diffusivity and conductivity are anisotropic quantities, being much smaller in the perpendicular direction. The mass dependence of the coefficients suggests that electrons and ions would diffuse at different rates. In practice, this is not the case; as one charge species tries to leave regions of high density ahead of the other, an electric field is built up. This ambipolar field holds the faster species back, maintaining quasi-neutrality, and both diffuse together.

The Fluid Picture Of Plasmas

Like ordinary gases, which are also large collections of particles, plasma can be treated like a fluid, although one that has significant electrical properties. The equations that govern the fluid-like properties are obtained by taking velocity integrals or moments of the Boltzmann equation, which describes the statistical evolution of a group of particles (the equation is essentially an equation of motion in phase space). In plasma physics, the relevant version of Boltzmann's equation (often called the Vlasov equation when collisions are rare) takes into account the effects of electromagnetic fields:

$$\frac{\partial f}{\partial t} + \boldsymbol{v} \cdot \nabla f + \frac{q}{m}(\boldsymbol{E} + \boldsymbol{v} + \boldsymbol{B}) \cdot \frac{\partial f}{\partial v} = \left(\frac{\partial f}{\partial t}\right)_{\mathrm{C}} \tag{15}$$

where f is the density of particles in six-dimensional phase space and $(\partial f/\partial t)_{\mathrm{C}}$ is a collision operator that describes the effects of coulomb interactions. q, m, and v are the charge mass and velocity of the particles under consideration. In many cases in plasma physics, collisions are ignored, though the fluid picture is only valid formally, when collisions are frequent enough to keep the mean free path much smaller than the system size. The zeroth moment of the Vlasov equation corresponds to mass conservation or continuity, the first moment corresponds to momentum conservation or force balance, and the second moment corresponds to energy conservation. In simplified form, the first two moments can be written

$$\frac{\partial nm}{\partial t} = -\nabla \cdot (nm\boldsymbol{v}) \tag{16}$$

$$\frac{\partial (nm\boldsymbol{v})}{\partial t} = nq(\boldsymbol{E} + \boldsymbol{v} \times \boldsymbol{B}) - \nabla \boldsymbol{P} \tag{17}$$

where $nm \equiv \rho$, the fluid mass density, and v is the fluid velocity and $\boldsymbol{P}$ is the pressure tensor. Note that the equation for each moment refers to the next higher moment, and the fluid velocity is needed to complete the continuity equation for example. To be useful, the set of equations must be closed, typically by making simplifying assumptions, like an equation of state. The moment equations combined with Maxwell's equations for electromagnetics form the basis for the fluid picture of plasmas called magnetohydrodynamics.

MAGNETOHYDRODYNAMICS

Magnetohydrodynamics (MHD) is the macroscopic fluid theory of plasmas. The equations that govern MHD are Maxwell's equations and moments of the Vlasov equation. These moments yield separate equations for ions and electrons, which are coupled through the fields generated and through collisions. It is common to use a single-fluid set of equations that can be derived by ignoring electron inertia, assuming that electron motion is fast compared to time scales of interest. This is equivalent to restricting our interest to times long compared to the electron cyclotron frequency and plasma frequency. A further simplification, appropriate in many cases, is made by ignoring resistive effects—that is, by assuming the plasma is a perfect conductor. The MHD equations are

$$\text{Continuity:} \quad \frac{\partial \rho}{\partial t} + \nabla \cdot (\rho \boldsymbol{v}) = 0 \tag{18}$$

$$\text{Momentum Balance:} \quad \frac{d\boldsymbol{v}}{dt} = \boldsymbol{J} \times \boldsymbol{B} - \nabla p \tag{19}$$

$$\text{Equation of State:} \quad \frac{dp}{dt} = -\gamma p \nabla \cdot \boldsymbol{v} \tag{20}$$

$$\text{Ampere's Law:} \quad \mu_0 \boldsymbol{J} = \nabla \times \boldsymbol{B} \tag{21}$$

$$\text{Faraday's Law:} \quad \frac{\partial \boldsymbol{B}}{\partial t} = \nabla \times \boldsymbol{E} \tag{22}$$

$$\text{Ohm's Law:} \quad \boldsymbol{E} + \boldsymbol{v} \times \boldsymbol{B} = \eta \boldsymbol{J} \tag{23}$$

$$\nabla \cdot \boldsymbol{B} = 0 \tag{24}$$

where ρ is the plasma mass density, p is the plasma pressure in SI units, and γ is the ratio of specific heats.

Equilibrium

In the fluid picture, magnetic confinement is achieved through the balance between plasma pressure and the magnetic force. At equilibrium the time derivatives vanish, leaving

$$\boldsymbol{J} \times \boldsymbol{B} = \nabla p \tag{25}$$

Figure 7 shows the geometrical relations between these quantities for a straight cylindrical plasma and B field. From Eq. (25), it is clear that both $\boldsymbol{J}$ and $\boldsymbol{B}$ must lie on surfaces of constant p. These surfaces are usually called flux surfaces and labeled with the enclosed magnetic flux. For a confined plasma, p will be a maximum near the axis and close to zero at the boundary. The current and field are related by Ampere's law, Eq. (21). For the case of a straight cylinder with a radial pressure gradient and no current parallel to B, $\boldsymbol{J} = J_\perp = \boldsymbol{B} \times \boldsymbol{\nabla p}/B^2$. This is called the diamagnetic current, and it arises from the imbalance in gyro-orbiting particles that is created by the pressure gradient. The pressure profile and parallel current can be considered free parameters in this equilibrium. Note that the magnetic field can be aligned in the z (axial) direction, with theta, or in some combination of the two. The essential pressure balance between the confining field and the plasma can be seen by substituting J from Ampere's law, which, after some vector algebra, yields the follow-

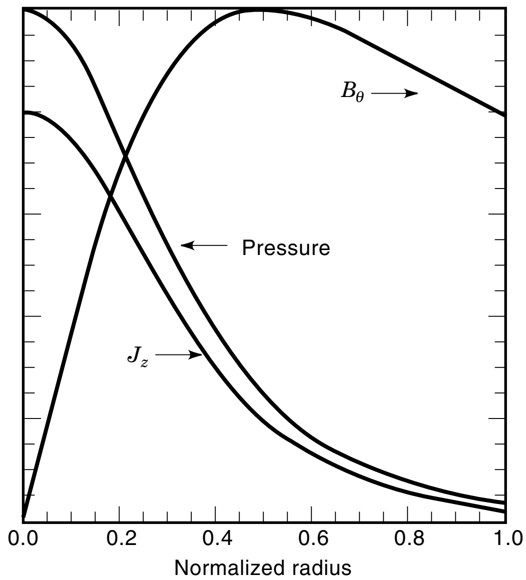

Figure 7. Sample profiles for the magnetic fields, currents, and plasma pressure for a simple MHD equilibrium, in this case a linear *Z* pinch. Named after the direction of the plasma current, the *Z* pinch actually predates the fusion energy program. It was first studied in 1934 by Bennet (24). The equilibrium requires balance between magnetic and plasma pressures.

ing for the case of straight field lines:

$$\nabla p = -\nabla\left(\frac{B^2}{2\mu_0}\right) \tag{26}$$

This relation suggests a definition for the normalized plasma pressure:

$$\beta = p\,\frac{2\mu_0}{B^2}$$

The importance of plasma pressure in the dynamics of a system is determined by beta.

As discussed previously, practical considerations require that a magnetic confinement device be toroidal. The toroidal geometry, illustrated in Fig. 4, adds two complications to the simple equilibrium just considered. First, the magnetic field must have both poloidal and toroidal components to cancel the single particle drifts. Second, in addition to radial force balance (from plasma pressure that tries to expand in the r direction), toroidal force balance must be considered as well. Two forces tend to expand the plasma in the R direction: one current-driven and one driven by the plasma pressure. Toroidal current exerts a hoop stress, as a result of the self-force between different current elements. The pressure imbalance arises because there is more surface area on the outside (large R) of the torus than the inside. Toroidal balance is achieved by the addition of a vertical magnetic field, which, when crossed with the toroidal current, produces a compensating force. In toroidal geometry, MHD equilibrium is calculated by the Grad–Shafranov equation (31,32). An example of an equilibrium in a toroidal device is shown in Fig. 8.

Stability

From the earliest studies into magnetically confined plasmas, researchers recognized that consideration of plasma equilibrium was not sufficient. Experimental plasmas could exhibit violent behavior sometimes losing their stored energy in a few microseconds. Further analysis showed that these plasmas were MHD-unstable: Like a ball sitting at the top of a hill, they were in a state of unstable equilibrium. Free energy for the instabilities comes from the plasma pressure and current. Pressure-driven modes exhibit "interchange" behavior: Parts of the fluid move toward the high-pressure region, while other parts move away. This phenomenon is analogous to the Rayleigh–Taylor instability that occurs when a glass of water is inverted. Current-driven instabilities often take the form of a kink; the plasma tries to twist itself into a corkscrew shape. Fortunately there are stabilizing forces that can come into play as the plasma moves away from equilibrium. Since the plasma is tied to magnetic field lines, these must be bent or compressed if the plasma is to move. Both processes require energy input and are thus stabilizing. Magnetic field curvature can be either stabilizing (when the pressure gradient is away from the center of curvature) or destabilizing. MHD stability is calculated by analyzing the effect of an infinitesimal displacement of the plasma. Destabilizing and stabilizing forces are summed up and found to move the plasma toward or away from equilibrium. Ideal MHD instabilities propagate at the Alfven velocity (see Table 1), which is on the order of 10^7 m/s for a fusion plasma, and therefore they must be avoided.

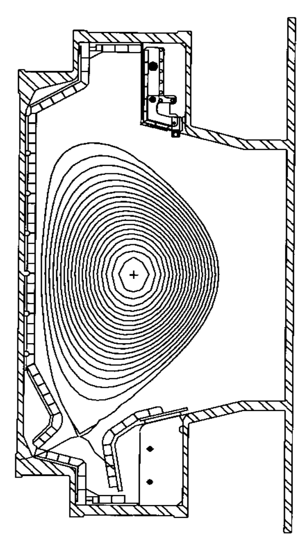

Figure 8. A poloidal cross section of MHD equilibrium in the Alcator C-Mod tokamak. The center of symmetry for the torus is on the left; the three-dimensional geometry is recovered by rotating the entire picture about that axis. The contours shown are for magnetic flux, which are also surfaces of constant magnetic pressure. In addition to the radial balance required in a linear system, toroidal force balance must also be preserved.

WAVES IN PLASMA

Just as ordinary fluids (like air) support sound waves, magnetized plasmas support a rich variety of wave phenomena. Waves are characterized by the displacements or perturbations that they produce in the medium that carries them. Plasma waves may perturb density and pressure as sound waves do, but are also able to alter electric and magnetic fields. A magnetic field breaks the isotropy of a plasma, with particle motions free in the parallel direction and inhibited in the perpendicular direction. Furthermore, there are at least two particle species in play (i.e., one or more types of ions and electrons), which can respond differently to waves owing to their very different mass. The general theoretical approach to describing waves in plasmas begins by linearizing the fluid equations about small perturbations, which are described as traveling waves, $e^{i(kx-\omega t)}$, where the wavenumber $k \equiv 2\pi/\lambda$. This process reduces the set of coupled partial differential equations to a system of ordinary algebraic equations that are then solved for $\omega(k)$. From this expression, called the dispersion relation, types of waves can be identified; also, group and phase velocities, regions of propagation, and resonances can all be calculated. The result is a complex family of waves whose description has filled many textbooks (33,34). Table 1 gives a greatly simplified summary of some of the more important wave types.

Waves are important for a number of reasons. They can be used for heating plasmas by launching waves from an external antenna, which then propagate into the plasma and then deposit their energy, usually by interacting with a natural plasma resonance. Waves are also generated spontaneously in plasmas, driven by the nonequilibrium state of a confined plasma. Temperature, density, and pressure gradients along with non-Maxwellian velocity distributions can all cause waves to grow. The waves, in turn, try to push the plasma back to a state of thermodynamic equilibrium, relaxing gradients and so forth. This can be a powerful mechanism for driving plasma transport and for destroying confinement.

Nonlinear Effects

While the approach to problems in plasma physics usually begins with linear analysis, plasmas themselves are intrinsically nonlinear. For example, consider self-diffusion where plasma particles diffuse via collisions with other plasma particles. The diffusion coefficients themselves are functions of the plasma density and temperature, rendering the diffusion of particles or heat nonlinear. Waves, when their amplitudes become large enough, affect the medium that is carrying them and thus change the propagation properties of the waves themselves. This mechanism also allows waves, which in linear theory are independent, to interact and to exchange energy. Finally, waves can interact with particles, whereby the wave fields strongly modify the particles' motions; conversely, particle motion can be converted into wave energy.

Nonlinear interactions allow large-scale, organized motions to be converted to smaller-scale, less organized motion. This cascade of energy between scales is characteristic of turbulence, a phenomenon which can be stimulated in any fluid. In a gas, a dimensionless quantity called the Reynolds number defines the regime where turbulence appears. $R \equiv UL/\nu$, where U is the fluid velocity, L is the system size, and ν is the fluid viscosity. For $R \gg 1$, viscosity is not sufficient to hold the fluid motion together into organized flow. For plasmas, the analogous dimensionless quantities are the magnetic Reynolds number $\equiv \mu_0 L V_T/\eta$, and the Lundquist number $\equiv \mu_0 L V_A/\eta$. (V_T is the thermal velocity and V_A is the Alfven velocity, defined in Table 1.) These are closely related, differing by $\sqrt{\beta}$, the square root of the ratio of plasma pressure to magnetic pressure. For a typical fusion plasma, the magnetic Reynolds number can approach 10^8. As a result, dynamically significant behavior can occur over a wide range in scale lengths, with collisional dissipation entering only on the smallest scales, where wave energy is degraded into thermal motion (heat). Typically, turbulent behavior can only be analyzed by simulation on powerful computers; however, some analysis is possible in terms of scaling relations. While the details of turbulent flows are terribly complex, overall, they must obey the basic conservation laws or symmetries of the the underlying physics.

TRANSPORT

Collisional Transport

Magnetic confinement can be understood from either the particle or fluid pictures of plasmas. In either case, nonideal ef-

Table 1. Properties of Some of the More Important Types of Waves Which Can Propagate in Magnetized Plasmas[a]

Wave Type	Common Name	Direction of Propagation	Polarization	Approximate Phase Velocity
Electrostatic ion wave	Ion accoustic wave	$\boldsymbol{k} \parallel \boldsymbol{B}_0$	$\boldsymbol{E}_1 \parallel \boldsymbol{B}_0$	$c_s = (kT_e/m_i)^{1/2}$ (ion sound speed)
Electrostatic electron wave	Plasma waves or Langmuir waves	$\boldsymbol{k} \parallel \boldsymbol{B}_0$	$\boldsymbol{E}_1 \parallel \boldsymbol{B}_0$	$v_e = (kT_e/m_e)^{1/2}$ (electron thermal speed)
Electromagnetic ion waves	Shear Alfven waves or simply Alfven waves	$\boldsymbol{k} \parallel \boldsymbol{B}_0$	$\boldsymbol{E}_1 \perp \boldsymbol{B}_0$	$v_A = B/(4\pi n_i m_i)^{1/2}$ (Alfven velocity)
	Compressional Alfven waves or magnetosonic wave	$\boldsymbol{k} \perp \boldsymbol{B}_0$	$\boldsymbol{E}_1 \perp \boldsymbol{B}_0$	v_A
Electromagnetic electron waves	O-wave	$\boldsymbol{k} \perp \boldsymbol{B}_0$	$\boldsymbol{E}_1 \parallel \boldsymbol{B}_0$	c (speed of light)
	X-wave	$\boldsymbol{k} \perp \boldsymbol{B}_0$	$\boldsymbol{E}_1 \perp \boldsymbol{B}_0$	c
	L-wave	$\boldsymbol{k} \parallel \boldsymbol{B}_0$	$\boldsymbol{E}_1 \perp \boldsymbol{B}_0$	c
	R-wave	$\boldsymbol{k} \parallel \boldsymbol{B}_0$	$\boldsymbol{E}_1 \perp \boldsymbol{B}_0$	c

[a] The common names given are for waves which propagate strictly parallel or perpendicular to the field; in general, propagation at arbitrary angles is possible and the nomenclature becomes less appropriate. The phase velocities listed are only approximate; the actual velocity, $v_\phi \equiv \omega/k$, is a function of frequency (ω) or wavenumber (k).

fects will tend to spoil confinement. Collisions cause particles to diffuse across the magnetic field by a random walk process. In the MHD model, the equivalent process is described by the diffusion of a conductive fluid through a magnetic field. Note that in ideal MHD, where resistivity is assumed to go to zero, the diffusion rate also goes to zero; the magnetic field is said to be frozen into the fluid. Taking Ohm's law from the equation for resistive MHD [Eq. (23)] and crossing it with B gives

$$\boldsymbol{E} \times \boldsymbol{B} + v_{\perp}|B|^2 = \eta \boldsymbol{J} \times \boldsymbol{B} \tag{27}$$

Combining this with the force balance equation [Eq. (19)] and solving for $v_{\perp}$, we obtain

$$v_{\perp} = -\eta \frac{\nabla p}{B^2} + \frac{\boldsymbol{E} \times \boldsymbol{B}}{B^2} \tag{28}$$

The first term describes plasma diffusion, while the second term is the fluid equivalent to the $\boldsymbol{E} \times \boldsymbol{B}$ particle drift. A little algebra will show, not surprisingly, that the diffusion rate for the fluid is the same as that derived above for particles. For a typical fusion plasma, this classical diffusion coefficient is on the order 10^{-3} m^2/s, far too small to present any problem for magnetic confinement.

The collisional diffusion coefficient, just calculated, is correct only for a plasma confined by a magnetic field that is straight and uniform. In a torus, diffusion is significantly enhanced by the particle drifts. The rotational transform forces the drifts to cancel when averaged over complete orbits; however, collisions can disrupt the orbit and cause the cancellation to be incomplete. The theory for collisional diffusion in axisymmetric toroidal geometry is called neoclassical transport and has been extensively developed for tokamaks (35). Figure 9(a) illustrates a tokamak cross section with the directions of the magnetic fields, plasma current (taken to be in the same direction as B_T in this example), and particle drift shown. Consider a particle with its parallel motion in the same direction as the plasma current, which follows the field lines in a right-hand spiral. In the poloidal cross section, such a particle will travel in a clockwise circle. The $\nabla \boldsymbol{B}$ drift will move such a particle off its flux surface, toward the plasma center while it is near the bottom of its orbit and away from the center while it is near the top. The maximum displacements occur when the particle is on the horizontal midplane, resulting in an orbit that is displaced outward, away from the torus center. This result holds whether the toroidal field and plasma current are in the same or in opposite directions. Ions circulating opposite to the plasma current will always be

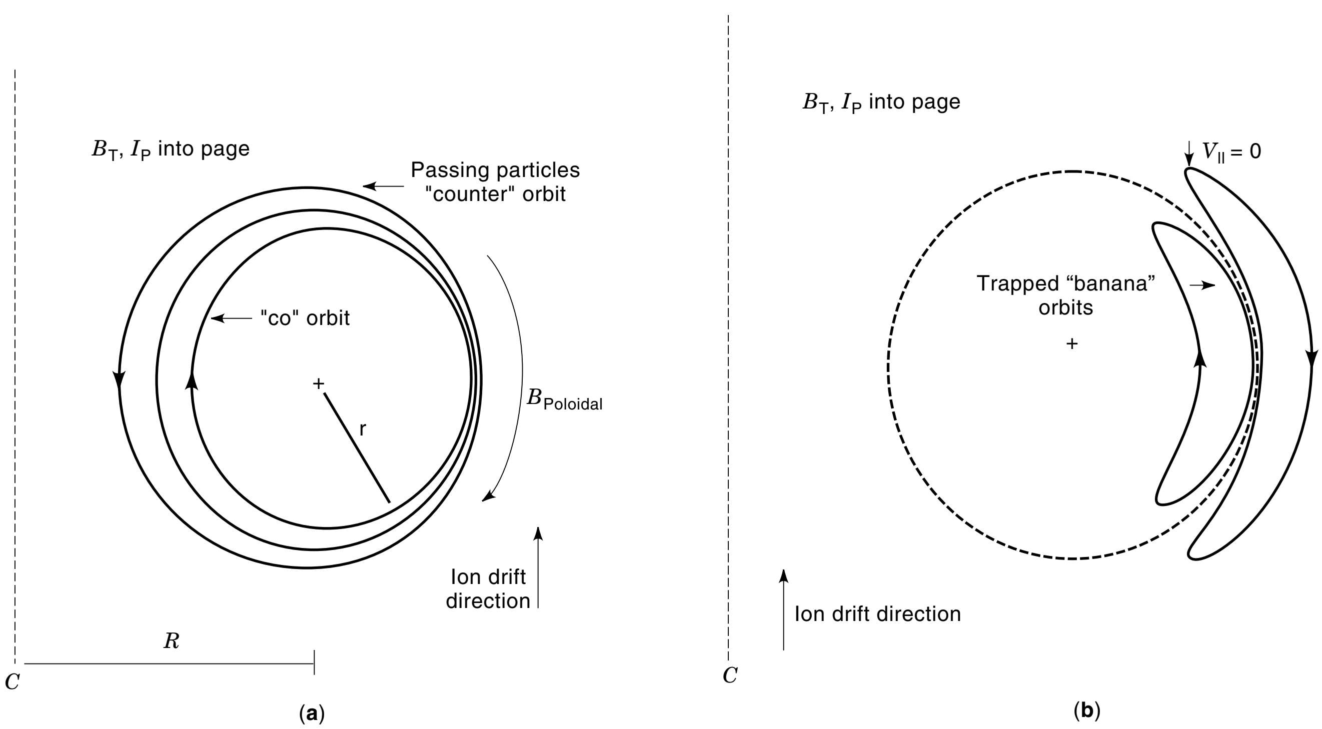

Figure 9. (a) In a torus, the $\nabla \boldsymbol{B}$ and curvature drifts result in particle orbits that do not follow magnetic field lines exactly. In this poloidal cross section, the projection of one set of field lines (flux surface) is shown by the dashed circle. The center of symmetry is on the left, and the coordinates R and r are shown. Simple application of Ampere's law shows that $B_{\text{Toroidal}} \propto 1/R$ thus $\boldsymbol{B} \times \nabla \boldsymbol{B}$ is vertical, upwards in this case, for positively charged ions. The poloidal field component gives a twist or helicity to the field lines. The result is that ions with velocities parallel to the plasma current (co) have orbits shifted out in major radius, R, relative to the flux surfaces while those moving in the opposite direction (counter) are shifted inward. (b) In the same geometry part (a), ions in so-called "banana" orbits are shown. These ions are trapped in the magnetic mirror created by the gradient in the toroidal field. Trapped particles are shifted off of flux surfaces even farther than the passing particles and thus can take large radial steps when they collide. These processes are the basis for the neoclassical theory of transport.

shifted inwards. The approximate size of that displacement δ_r, can be calculated:

$$\delta_r = v_D \tau \quad (29)$$

where $\tau \approx qR/v_T$ is the period the particle takes to complete a poloidal orbit. (In a low-aspect-ratio tokamak with $a/R \ll 1$, $q = rB_T/RB_P$ and is typically in the range 1 to 5.) Using Eq. (10) for the $\nabla \boldsymbol{B}$ drift velocity and noting that $\nabla \boldsymbol{B}/B = 1/R$, the orbit shift is given by

$$\delta_r = v_T \rho_i \frac{\nabla \boldsymbol{B}}{B} \frac{qR}{v_T} = q\rho_i \quad (30)$$

Thus, the stepsize caused by collisions is increased by a factor of q and diffusion by q^2. The effects of toroidal geometry are even more pronounced on another class of particles, those with enough perpendicular energy to be trapped by the tokamak's inhomogeneous toroidal field. The magnetic field experienced by a particle in a tokamak varies by a factor on the order r/R as it moves. Those with $v_\parallel/v_\perp \leq \sqrt{\epsilon}$ will be reflected by the stronger magnetic field on the inner part of their trajectory. These trapped particles execute banana shaped orbits as shown in Fig. 9(b). The width of the bananas are larger than δ_r by $\sqrt{(R/r)}$, and they diffuse even faster than circulating particles. Overall, neoclassical diffusion coefficients are on the order 50 times larger than the classical values for a plasma in a tokamak. Plasma resistivity is reduced by neoclassical effects, since trapped particles do not complete circuits of the torus and cannot carry current.

For nonaxisymmetric plasmas, collisional diffusion can be larger still (36). In an axisymmetric system, particles are governed by conservation of canonical angular momentum $p_\Phi = mv_\Phi R + eA_\Phi R$, where A is the vector potential of the magnetic field. As long as the particle's kinetic momentum is not too large, they are constrained to stay close to flux surfaces, which are also surfaces of constant RA_Φ. (This is, in fact, an alternative picture for describing particle orbits in a torus.) This constraint is absent if the system lacks axisymmetry where certain classes of particles can make large radial excursions or leave the plasma entirely without undergoing any collisions. The loss rate for the plasma as a whole is then governed by the rate at which the hole in the velocity distribution function is filled in. These effects are most important in intermediate collisionality regimes, where particles on lost orbits can travel significant distances without colliding, but where collisions are still able to fill in the losses from the background plasma. For stellarators, whose helical field breaks the axisymmetry, these losses can dominate transport; modern stellarators are carefully designed to minimize their magnitude. The fields of nominally axisymmetric devices, like a tokamak, have a small asymmetry due to the finite number of toroidal coils. This periodic ripple can cause significant loss of energetic particles, particularly those with mostly perpendicular energy, since parallel motion tends to average out the asymmetries.

Anomalous Transport

Even with neoclassical corrections, collisional transport is not fast enough to cause serious concern (at least in axisymmetric devices); even small machines could have confinement times longer than 1 s. In experiments, energy confinement was almost always found to be much worse than that calculated from the collisional theories, often by a factor of 100 or more (37). At the outset it was suspected that this anomalous transport had its origins in small-scale plasma instabilities (usually called microinstabilities), but it took several decades before scientists could develop a quantitative understanding of the phenomenon, and even now it is far from complete (38). Experimentalists have developed techniques for drastically reducing anomalous transport, sometimes to nearly the neoclassical levels (17–20), though so far these have been only for transient situations.

Waves, driven by the plasma's free energy, can cause transport by two basic mechanisms. First, magnetic perturbations can break up magnetic flux surfaces, allowing particles to make radial excursions as they follow the field lines. While large-scale magnetic perturbations driven by MHD instabilities destroy confinement almost instantly, low-amplitude waves can result in enhanced transport. Because of their higher velocity, electrons follow magnetic perturbations more readily and would carry most of the heat in this case. The second mechanism, and the one believed responsible for anomalous transport in most experiments, results from the electrical component of plasma instabilities. These are typically low-frequency waves ($\omega \ll \omega_c$), which have a fluctuating electric field as part of their dynamics. Differences in electron and ion motion, due to their different mass, cause charge separation and result in regions of positive and negative electric potential, each of which is then surrounded by fluid rotating in the resulting $\boldsymbol{E} \times \boldsymbol{B}$ drift (Fig. 10). When combined with

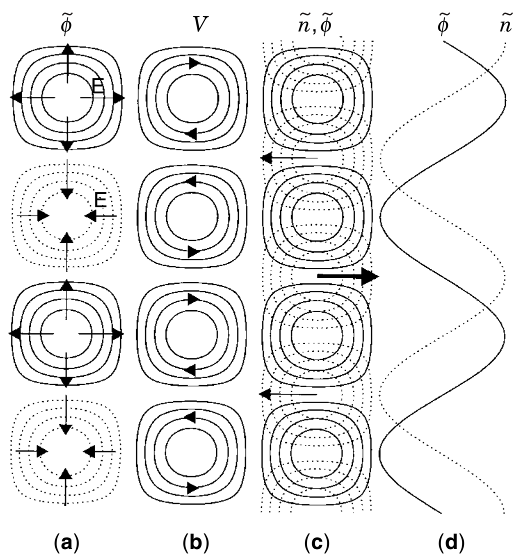

Figure 10. Particle and energy can be transported by plasma fluctuations. This series of pictures shows how particle fluxes arise from electrostatic oscillations. The magnetic field is assumed to be in the direction directly out of the page. Part (a) shows the fluctuating potential $\tilde{\phi}$, with positive $\tilde{\phi}$ shown by solid lines and negative $\tilde{\phi}$ shown by dotted lines. The potential gradients result in electric fields, which lead to $\boldsymbol{E} \times \boldsymbol{B}$ drifts and the fluctuating flow patterns shown in (b). In (c), $\tilde{\phi}$ is overlaid with a fluctuating density pattern, $\tilde{n}$, shown in dotted lines. A profile through the center of the pattern is shown in (d). With the relative phase of $\tilde{\phi}$ and $\tilde{n}$ as given, the flows are strongest to the right where the density is highest. The result is net particle flux to the right. If the relative phase of $\tilde{\phi}$ and $\tilde{n}$ were shifted by π, the net transport would be in the opposite direction.

density or temperature perturbations from the instability, net particle and energy transport can occur.

Theories of anomalous transport try to answer three questions. First, what is the nature of the plasma waves and the conditions that cause them to grow? Second, What is the spectral distribution of the waves in frequency and wavelength? Third, how much transport is caused? The source of microinstabilities is usually analyzed by linear theory—that is, by comparing destabilizing and stabilizing terms with respect to small-amplitude perturbations. Wave–particle interactions must often be added to get an accurate model for the dynamics. Linear theories can predict the conditions under which these waves will grow, as well as the exponential growth rate for small fluctuations. The growth rate can be determined as a function of k and ω, suggesting a linear spectrum that is largest at those k and ω where the growth rate is highest. For finite-amplitude waves, nonlinear interactions will modify the instability as waves of different sizes exchange energy. On very short wavelength scales, linear and nonlinear damping mechanisms provide an energy sink as wave energy is converted to thermal particle motion. The fully evolved nonlinear, turbulent spectrum can be quite different from the one predicted by linear theory and requires powerful computers for its calculation. Particle and energy fluxes, driven by the turbulence, can then be determined by constructing appropriate phase-averaged quantities. For example, the particle flux from electrostatic instabilities is calculated from

$$\Gamma = \frac{\langle \tilde{n}\tilde{E} \rangle}{B} = \frac{\langle \tilde{n}^2 \rangle^{1/2} \langle \tilde{E}^2 \rangle^{1/2} \sin\theta}{B} \tag{31}$$

Where $\tilde{n}$ and $\tilde{E}$ are the fluctuating components of those two quantities, θ is their relative phase and $\langle\,\rangle$ represents a phase average. While fluctuations in plasmas, similar to those predicted by theory, are readily observed, conclusive evidence linking them to anomalous transport has been difficult to obtain. In the plasma edge, electrostatic probes can measure all the required fluctuating quantities along with the their relative phases. In the plasma core, these measurements are much more difficult. Density fluctuations are measured routinely, though only over a limited range of wavenumbers, while $\tilde{E}$ and $\tilde{B}$ can scarcely be measured at all. The computation of the turbulence spectra is also fraught with difficulties. In realistic geometries, three-dimensional (3-D) simulations may be necessary and substantial approximations must be made to allow the calculation to complete on even the most powerful machines. Runs taking over 1000 h on advanced supercomputer are not unusual. Thus progress is incremental, with experimental measurements and theoretical calculations used to guide each other to successively better models.

HEATING, CURRENT DRIVE, AND FUELING

The previous section considered the dissipation mechanisms for energy, mass, and current. In a fusion device, these must be balanced by sources, namely heating, fueling, and current drive. In an ignited reactor, the heat source would be internal, from the fusion reactor itself. However, even in this case, the reactor would need an external source of heat to bring the plasma to temperature. The present generation of experiments, of course, are entirely dependent on external heating. Any device with finite particle confinement time needs a mechanism to replace or recycle particles lost at the boundary. Of course, a reactor would also need a source of fuel to replace hydrogen isotopes as they are converted to helium. Finally, those confinement schemes, which rely on currents flowing in the plasma, must find a method for sustaining that current against resistive losses or operate only in a pulsed mode.

Heating Methods

Ohmic Heating. For confinement schemes like the tokamak, which rely on large currents flowing in the plasma, one source of heat is readily at hand: resistive or ohmic heating. The plasma currents are driven inductively, with voltage appearing as the result of time-varying magnetic flux, which, in turn, is driven by external coils. Resistive dissipation of the plasma current provides the heating source. The local source rate is equal to ηj^2. The total plasma current is usually limited by MHD stability, resulting in heating proportional to $\eta \propto 1/T_e^{3/2}$. Thus ohmic heating becomes less and less effective as the temperature increases. Tokamaks with ohmic heating alone can reach electron temperatures of several kiloelectronvolts, though the ions are typically much cooler. While there is no a priori reason why ohmic heating alone could not be large enough to reach ignition, extrapolation from experiments suggests that it would not be sufficient in any practical device.

Neutral Beam Heating. Intense beams of neutral atoms have been used successfully for heating fusion plasmas since 1971 (39–41). Neutrals are used because charged particle beams, though they are easily produced, cannot penetrate magnetic fields. Neutral injectors (42) have three principal components: a plasma source, where gas (typically a hydrogen isotope) is ionized; an accelerator, where plasma ions are electrostatically extracted and accelerated; and a neutralizer, where the charged ions interact with neutral gas, picking up electrons to become neutral atoms. Atomic cross sections limit this approach to beam energies less than 150 keV. Beam currents are limited by space charge effects in the extractor/accelerator system to about 0.5 A/cm^2. Injectors, however, can be quite large, enabling multi-MW systems to be assembled. Major fusion experiments may have more than 20 MW of neutral beam heating available. Neutral beam injectors have been used on virtually every type of magnetic confinement device.

Once inside the plasma, the neutral beam is quickly ionized and the ion energy is converted to heat. Experiments have shown that these processes are essentially classical—that is, dominated by collisional rather than anomalous processes. It is believed that this is because the gyro radius of beam ions is much larger than the fine scale turbulence that is the cause of anomalous transport for the slower thermal ions. The large orbits effectively average out the fluctuations. Beam penetration is limited by atomic processes, principally electron and ion impact ionization and charge exchange, with ion impact ionization dominating at the highest energies available from conventional injectors, where the cross section is about 10^{-20} m^2. Thus in a typical fusion plasma with a density of 1×10^{20}/m^3, the beams will penetrate about 1 m. This would be problematic for proposed devices that might have cross sections which are several meters in radius, or for very high-density devices. Higher energies can only be produced in so-called negative ion sources, in which hydrogen atoms with two electrons are created, extracted, and accelerated. The second electron is only weakly bound, and the system is easily neutralized. Negative ion sources are experimental, but have produced beams with energies up to 500 keV (43).

Radio-Frequency Heating. In radio-frequency (RF) heating, energy is added to the plasma via electromagnetic waves. A wide variety of approaches have been tested, differing mainly in the frequency of the waves employed. Each shares certain common features and faces similar issues, namely, RF generation, launching, coupling, propagation, and dissipation. Efficient, high-power RF sources are available over a wide range in frequency from a few hundred kilohertz to over 100 GHz. (The limitation at the high end is particularly important because this is the frequency range for electron gyro motion; f_c = 28 GHz/T.) RF power can easily be transmitted by coaxial conductors or in waveguides to launching structures, situated near the edge of the plasma. For low frequencies, antennas are the appropriate launcher, with horns or windows used for microwaves. Coupling to the plasma is not as straightforward. Recall that due to rapid response of the electrons in a plasma, transverse electromagnetic waves below the plasma frequency are reflected rather than transmitted. In RF heating schemes, the goal is to launch a plasma wave that is able to propagate. Since most plasma waves do not propagate in a vacuum and since the antenna in general is not in direct contact with the plasma, there is typically an evanescent (nonpropagating) layer through which the wave must tunnel. The type of plasma wave employed will depend on plasma properties and the frequency of the launched wave. Finally, the waves must be made to deposit their energy into plasma particles. Depending on the heating scheme, this takes place via various wave–particle resonances, in which the particles are accelerated by the wave field and then give up their energy by collisions to the background plasma. Overall, the physics of wave propagation, mode conversion, and damping can be quite complex and it remains an active area of research. Three frequency ranges show the greatest promise for RF wave heating: ion cyclotron waves at frequencies of 20 MHz to 120 MHz; lower-hybrid waves at 1 GHz to 5 GHz; and electron cyclotron waves at 50 GHz to 250 GHz.

In the ion-cyclotron range, antennas are generally used to launch the waves since the free space wavelength is 4m to 25 m, which is large compared to the size of the plasma being heated. The antenna, a current-carrying poloidal loop, drives a compressional Alfven wave that tunnels through a thin evanescent region at the plasma edge and then propagates across the plasma until it reaches the ion cyclotron layer (the radius where the RF frequency equals the ion cyclotron frequency). Efficient wave–ion coupling is realized only when the wave has the proper polarization relative to ion cyclotron motion. This is achieved by resonating with a minority ion species (minority heating) or by launching an RF wave at twice the cyclotron frequency of the majority ion (second harmonic heating). Both have been employed successfully in experiments (44,45). Figure 11 shows a set of ion cyclotron range of frequencies (ICRF) antennas installed in a tokamak.

The lower-hybrid frequency is $\omega_{\rm LH} \approx \omega_{\rm pi}\sqrt{(1 + \omega_{\rm pe}^2/\omega_{\rm ce}^2)}$, where $\omega_{\rm pi}$ is defined by analogy to the electron plasma frequency as $\omega_{\rm pi} = \sqrt{(n_i Z^2 e^2/m_i)}$. The free space wavelength is on the order of 0.1 m, so fundamental mode waveguides are typically used to carry and launch the waves, with the electric field polarized parallel to the magnetic field of the plasma. As in the previous case, the waves must tunnel through a thin evanescent layer before propagating in the plasma. To reach the lower-hybrid resonance, the waves must satisfy an accessibility condition:

$$\frac{k_{\parallel} c}{\omega} > \left(\sqrt{1 + \frac{\omega_{\rm pe}^2}{\omega_{\rm ce}^2}} \right)_{\omega=\omega_{\rm LH}} \tag{32}$$

To produce this spectrum, waveguide arrays are used, with the waves' phase appropriately shifted from one waveguide to the next. The waves can damp at the lower-hybrid layer by resonance with the ions or electrons, depending on details of the wave physics. Lower-hybrid heating experiments have been carried out with mixed results, mainly on smaller-scale experiments (46,47).

The highest-frequency waves used for heating are in the electron cyclotron region. Here, strong RF sources are available only up to about 100 GHz, limiting the scheme to devices with fields less than 3 T. The wavelengths involved are only a few millimeters, and overmoded waveguides or quasi-optical techniques can be employed for transporting and launching the waves. Coupling and propagation are relatively simple: The plasma carries two types of electromagnetic waves that propagate perpendicular to the field at these frequencies, one polarized with $E \| B$ (ordinary or O mode) and the other with $E \perp B$ (extraordinary or X-mode). The waves can be cut off when the wave frequency approaches the plasma frequency, so the scheme is limited to relatively low densities. By using higher electron cyclotron harmonics for the resonant absorption, the method can be applied to higher-density plasmas, but source availability and the weaker damping limit this to the first few harmonics only.

Current Drive

Plasma currents, which are necessary in many types of confinement schemes, are typically driven inductively, by swinging the flux in external coils. This approach is quite effective for pulsed experiments, but the flux swing is limited by the current carrying capacity of the coils. The induced voltage can only be sustained for a finite amount of time, after which the coils must be recharged. At high temperatures, the plasma resistivity can be very low and inductive currents can be sustained for quite long pulses—up to 30 s in some experiments. To achieve steady state, which is desirable because it reduces cyclic stresses, noninductive current drive methods must be employed. In certain circumstances, the plasma itself can generate most of the required current, tapping into free energy from the plasma pressure gradient. This phenomenon, called bootstrap current, can be understood by considering the banana orbits shown in Fig. 9(b). Note that the outer segment of these ion orbits is always in the direction parallel to the plasma current (co), whereas the inner segment is always in the antiparallel direction ("counter"). Since the density is higher near the center of the plasma than on the outside, the number of particles traveling in the "co" direction will outnumber those in the counter direction. The current carried by these particles can be estimated by first noting that for a

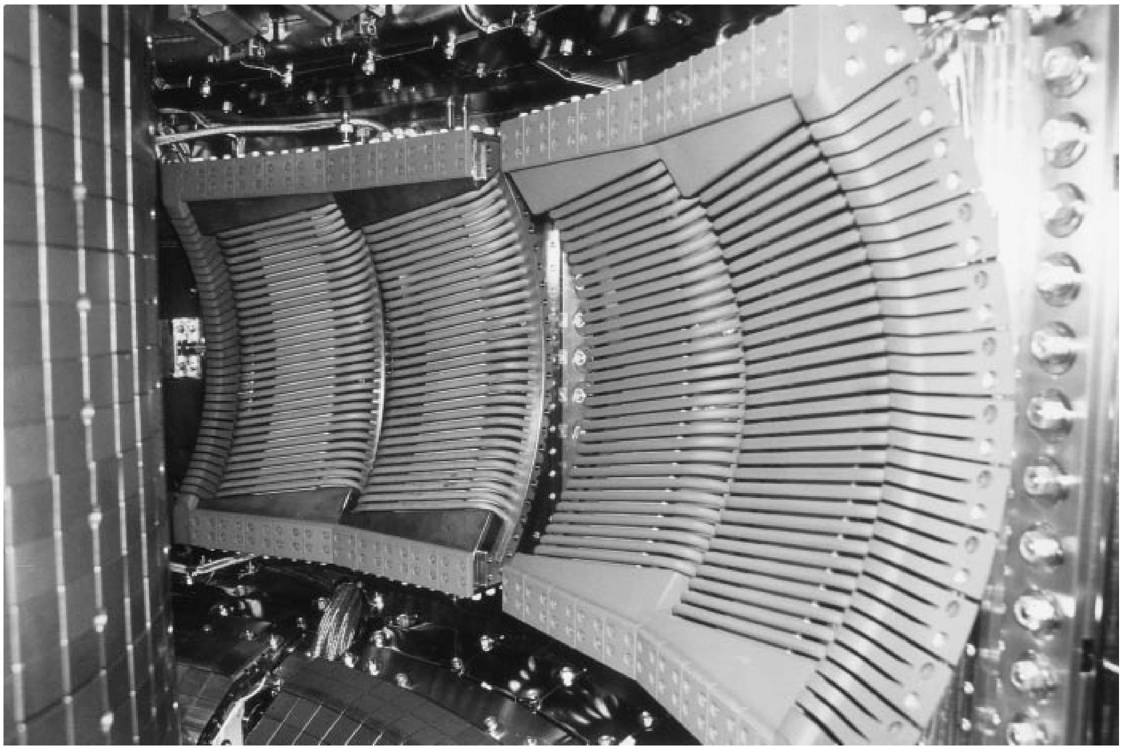

Figure 11. An antenna used for ICRF heating installed in the Alcator C-Mod tokamak. The current straps, which generate the RF fields, can be seen behind a Faraday shield which keeps plasma from interfering with its operation.

collisionless plasma, the fraction of trapped particles is $\epsilon^{1/2}$ and that they have an average parallel velocity $\langle v_\parallel \rangle$ on the order $\epsilon^{1/2} v_T$. The banana width is $\delta \approx \epsilon^{-1/2} q\rho$, from which the differential number of "co" and "counter" going particles can be inferred:

$$\Delta_n \approx e^{1/2}\delta \frac{dn}{dr} = q\rho \frac{dn}{dr} \tag{33}$$

Combining these results, the bootstrap current carried by trapped particles is

$$j = ev_\parallel \Delta_n = \frac{q\epsilon^{1/2}T}{B}\frac{dn}{dr} \tag{34}$$

Actually, somewhat more bootstrap current is carried by passing particles. This results from a distortion of the passing particle distribution function that is caused by their interaction with trapped particles (48). In theory, almost all the required current can be generated by this process, however, the bootstrap current profile may not be optimal from the point of view of MHD stability. Another method used for noninductive current drive is the application of RF waves with phase velocities parallel to the direction of the desired current. These waves can interact resonantly with electrons traveling at the same velocity, accelerating them in the wave field. Waves in the lower-hybrid frequency range can be employed for this purpose, though the launched spectrum must be modified from that used for heating (49,50). Electron cyclotron waves can drive current by differentially heating electrons traveling in the "co" and "counter" direction, using the resonance condition to separate the two populations via their Doppler shifts. This effect is only strong for those electrons with velocities much higher than the average thermal velocity, leading to relatively low efficiency in most cases.

Fueling

In order for a fusion device to run much longer than a confinement time, some mechanism for replacing lost plasma must be found. Ionized particles leaving a plasma in a confined experimental volume are neutralized quickly when they touch the vacuum system walls. A substantial fraction are implanted in the surface layers of the wall, while at the same time other gas molecules are liberated by the impact of heat and particles on the surface. In equilibrium, there is a balance between these two processes, establishing a steady-state neutral gas pressure in the region between the plasma and the wall. Gas impinging on the plasma is disassociated and rapidly ionized, creating a strong source at the plasma boundary. The width of the source region varies with plasma density and temperature, but is typically a few millimeters to a few centimeters, much smaller than the plasma cross section. Most of these new ions are quickly lost again, but some are able to move up the density gradient into the core plasma, by processes that are only partially understood. A collisional process, the neoclassical or Ware pinch, can account for this inward particle flux in some cases; however, in many others, it is found to be too small. Anomalous pinches can be driven by some of the same processes that cause outward transport; in effect, a heat engine is created with outward energy flow driving inward particle flow against the gradient. Basic thermodynamic considerations put limits on how large these fluxes can be.

While gas fueling works well in current experiments, the lack of a comprehensive theory for the process has motivated researchers to search for alternate techniques. Neutral beams, which are often used for heating, also supply particles to the plasma. In some experiments these can dominate the source from gas fueling; however, it does not seem to be a method that could extrapolate to a reactor. Deep fueling requires high-energy beams, but it is too expensive to supply all the plasma particles with that much energy. Another alternative is to inject fuel in the form of small cryogenic pellets (51). As macroscopic objects, they can penetrate much farther into the plasmas than individual molecules. Extrapolation is also an issue here, since injection velocity seems to be limited by the tensile strength of frozen deuterium, to a few kilometers per second. Pellets at these velocities are very effective for central fueling of current machines, but would not penetrate deeply into a reactor plasma. Recent experiments suggest that it may be possible to take advantage of certain MHD instabilities to augment this penetration, however (52). Central fueling, whether from beams or pellets, has additional benefits. Gas fueling tends to produce very flat density profiles, while fusion yields could be increased with peaked densities. Furthermore, it has been demonstrated that plasmas with peaked density profiles from central fueling can have dramatically reduced energy transport (17,53).

BIBLIOGRAPHY

1. A. S. Bishop, *Project Sherwood, the U.S. Program in Controlled Fusion,* Reading, MA: Addison-Wesley, 1958.
2. J. L. Bromberg, *Fusion: Science Politics and the Invention of a New Energy Source,* Cambridge, MA: MIT Press, 1983.
3. R. Herman, Fusion, *The Search for Endless Energy,* Cambridge, UK: Cambridge Univ. Press, 1990.
4. K. M. McGuire, TFTR Team, *Phys. Plasmas,* **2**: 2176, 1995.
5. A. Gibson, JET team, *Phys. Plasmas,* **5**: 1997.
6. J. D. Lawson, *Proc. Phys. Soc. B,* **70**: 6, 1957.
7. H. Eubank, PLT Team, *Proc. 7th Int. Conf. Plasma Phys. Controlled Nucl. Fusion Res.,* Innsbruck, 1978, Vol. I, 1979, p. 177.
8. M. Greenwald, Alcator Team, *Phys. Rev. Lett.,* **53** (4): 352, 1984.
9. K. Ushigusa, JT-60 Team, Plasma Physics and Controlled Nuclear Fusion Research, *Proc. 16th Int. Conf.,* Montreal, 1996; Vol. I, 1997, p. 37.
10. JET Team, *Proc. of 16th Int. Conf. Plasma Phys. Controlled Nucl. Fusion Res.,* Montreal, 1996; vol. I, 1997, p. 57.
11. K. M. McGuire, TFTR Team, *Proc. 16th Int. Conf. Plasma Phys. Controlled Nucl. Fusion Res.,* Montreal 1996, Vol. I, 1997, p. 19.
12. A. S. Bishop and E. Hinnov, *Proc. 2nd Int. Conf. Plasma Phys. Controlled Nucl. Fusion Res.,* Culham, 1966, Vol. II, 1967, p. 673.
13. F. Wagner, Wendelstein Team, *Plasma Phys. Controlled Fusion,* **36**: A61, 1994.
14. F. Sano, Heliotron Group, *Nucl. Fusion,* **30**: 81, 1990.
15. L. A. Artsimovich et al., English translations of papers from *Proc. 3rd Int. Conf. Plasma Phys. Controlled Nucl. Fusion Res.,* Novosibirsk, 1968, *Nucl. Fusion Suppl.,* **17**: 1969.
16. N. J. Peacock et al., *Nature,* **224** (5218): 488, 1969.
17. M. Greenwald, Alcator Team, *Proc. 11th Int. Conf. Plasma Phys. Controlled Nucl. Fusion Res.,* Kyoto, 1986, Vol. I, 1987, p. 139.
18. Y. Koide et al., *Phys. Rev. Lett.,* **72**: 3662, 1994.
19. F. M. Levinton et al., *Phys. Rev. Lett.,* **75**: 4417, 1995.
20. E. J. Strait et al., *Phys. Rev. Lett.,* **75**: 4421, 1995.
21. H. A. B. Bodin and D. E. Evans, *Nucl. Fusion,* **25**: 1305, 1985.
22. D. J. Den Hartog et al., Euchimoto, *Proc. 16th Int. Conf. Plasma Phys. Controlled Nucl. Fusion Res.,* Montreal, 1996, Vol. II, 1997, p. 83.
23. M. Tuszewski, *Nucl. Fusion,* **28**: 2033, 1988.
24. W. H. Bennet, *Phys. Rev.,* **45**: 890, 1934.
25. E. M. Little et al., *Proc. 3rd Int. Conf. Plasma Phys. Controlled Nucl. Fusion Res.,* Novosibirsk, 1968, Vol. II, 1969, p. 555.
26. J. A. Van Allen et al., *Jet Propulsion,* **28**: 588, 1958.
27. M. S. Ioffe et al., (English translation), *Sov. Phys.—JETP,* **13**: 27, 1961.
28. T. C. Simonen, *Nucl. Fusion,* **25**: 1205, 1985.
29. P. C. Stangeby and G. M. McCracken, *Nucl. Fusion,* **30**: 1225, 1990.
30. G. F. Matthews, *J. Nucl. Mater.,* **104**: 220–222, 1995.
31. H. Grad and H. Rubin, *Proc. 2nd United Nations Int. Conf. Peaceful Uses of Atomic Energy,* United Nations, Geneva, Vol. 31, 1958, p. 190.
32. V. D. Shafranov, *Sov. Phys.—JETP,* **26**: 682, 1960.
33. T. H. Stix, *Waves in Plasmas,* New York: American Institute of Physics, 1992.
34. R. A. Cairns, *Radiofrequency Heating of Plasmas,* Bristol, UK: Adam Hilger, 1991.
35. F. L. Hinton and R. D. Hazeltine, *Rev. Mod. Phys.,* **48**: 239, 1976.
36. L. M. Kovrizhnykh, *Nucl. Fusion,* **24**: 851, 1984.
37. P. C. Liewer, *Nucl. Fusion,* **25**: 543, 1985.
38. J. W. Connor and H. R. Wilson, *Plasma Phys. Controlled Fusion,* **36**: 719, 1994.
39. K. Berkner et al., *Proc. 4th Int. Conf. Plasma Phys. Controlled Nucl. Fusion Res.,* Madison, 1971, Vol. II, 1971, p. 707.
40. J. G. Cordey et al., *Nucl. Fusion,* **15**: 441, 1975.
41. L. A. Berry, ORMAK Team, *Proc. 5th Int. Conf. Plasma Phys. Controlled Nucl. Fusion Res.,* Tokyo, 1974, Vol. I, 1975, p. 101.
42. W. S. Cooper, K. H. Berkner, and R. V. Pyle, *Nucl. Fusion,* **12**: 263, 1972.
43. K. Watanabe et al., *Proc. 14th Int. Conf. Plasma Phys. Controlled Nucl. Fusion Res.,* Wurtzburg, 1992, Vol. III, 1993, p. 371.
44. Equipe TFR, *Plasma Phys.,* **24**: 615, 1982.
45. D. Q. Hwang, PLT Team, *Proc. 9th Int. Conf. Plasma Phys. Controlled Nucl. Fusion Res.,* Baltimore, 1982, Vol. II, 1983, p. 3.
46. J. J. Schuss, Alcator Team, *Nucl. Fusion,* **21**: 427, 1981.
47. C. Gormezano et al., *Nucl. Fusion,* **21**: 1047, 1981.
48. R. J. Bickerton, J. W. Connor, and J. B. Taylor, *Nature Phys. Sci.,* **229**: 110, 1971.
49. S. Bernabei, PLT Team, *Phys. Rev. Lett.,* **49**: 1255, 1982.
50. M. Porkolab, Alcator Team, *Proc. 9th Int. Conf. Plasma Phys. Controlled Nucl. Fusion Res.,* Baltimore, 1982, Vol. I, 1983, p. 227.
51. S. L. Milora et al., *Nucl. Fusion,* **35**: 657, 1995.
52. P.T. Lang et al., *Phys. Rev. Lett.,* **79**: 1487, 1997.
53. B. J. Tubbing, JET Team, *Nucl. Fusion,* **28**: 827, 1988.

Reading List

G. L. Baker and J. P. Gollub, *Chaotic Dynamics,* Cambridge, UK: Cambridge Univ. Press, 1990. A readable introduction to nonlinear dynamics.

G. Bateman, *MHD Instabilities,* Cambridge, MA: MIT Press, 1978.

F. Chen, *Introduction to Plasma Physics,* New York: Plenum Press, 1984.

P. C. Clemmow and J. P. Dougherty, *Electrodynamics of Particles and Plasmas,* Reading, MA: Addison-Wesley, 1990.

R. O. Dendy (ed.), *Plasma Physics, An Introduction Course,* Cambridge, UK: Cambridge Univ. Press, 1993.

J. Freidberg, *Ideal Magnetohydrodynamics,* New York: Plenum Press, 1987.

R. J. Goldston and P. H. Rutherford, *Introduction to Plasma Physics,* Bristol: Institute of Physics, 1995.

I. H. Hutchinson, *Plasma Diagnostics,* Cambridge, UK: Cambridge Univ. Press, 1987. An introduction to the experimental techniques used for making measurements of plasmas.

N. A. Krall and A. W. Trivelpiece, *Principles of Plasma Physics,* New York: McGraw-Hill, 1986.

W. Lochte-Holtgreven, *Plasma Diagnostics,* Amsterdam: North-Holland, 1968.

K. Miyamoto, *Fundamentals of Plasma Physics and Controlled Fusion,* Tokyo: Iwanami Book Service Center, 1997.

L. Spitzer, *Physics of Fully Ionized Gases,* New York: Wiley, 1962. An introduction to the field from one of its founders.

T. H. Stix, *Waves in Plasmas,* New York: American Institute of Physics, 1992. A formal survey of wave phenomena in plasmas.

D. G. Swanson, *Plasma Waves,* New York: Academic Press, 1989.

J. Wesson, *Tokamaks,* Oxford: Oxford Science Publications, 1987.

Martin Greenwald
Massachussetts Institute of Technology